



# Glycoconjugates of choroidal neovascular membranes in age-related macular degeneration

Robert F. Mullins, Michael A. Grassi, Jessica M. Skeie

Center for Macular Degeneration, Department of Ophthalmology and Visual Science, The University of Iowa Carver College of Medicine, Iowa City, IA

**Purpose:** Choroidal neovascularization (CNV) is a complication of multiple eye diseases, including age-related macular degeneration, that usually results in irreversible vision loss. It is characterized by proliferation and growth of choroidal blood vessels through Bruch's membrane into the subpigment epithelial and/or subretinal space. The purpose of this study was to characterize the carbohydrate groups associated with CNV by lectin histochemistry.

**Methods:** Frozen sections from three human eyes with CNV (two fixed eyes and one unfixed eye) were prepared. Sections containing choroidal neovascular membranes were incubated with a battery of biotinylated lectins directed against a number of distinct oligosaccharide moieties. Lectin labeling of the vessels in CNV was visualized with avidin-Texas red.

**Results:** Several carbohydrate groups were preferentially associated with the vascular elements in CNV. Glycoconjugates that react with lectins derived from wheat germ, soybean, and hairy vetch seed (sWGA, SBA, and VVA, respectively) all showed reactivity with CNV vessels that was higher than the labeling of the surrounding matrix. SBA and sWGA also reacted with CNV vessels at low concentrations at which normal retinal and choroidal vessels were largely unlabeled.

**Conclusions:** Choroidal neovascular membranes possess a distinct set of carbohydrate moieties. These data may be valuable in understanding endothelial cell biology in CNV.

A final common pathway and source of vision loss for many diseases is choroidal neovascularization (CNV) and its subsequent disciform scarring [1]. In this condition, the choroidal vasculature penetrates Bruch's membrane, resulting in injury to the retinal pigment epithelium and photoreceptor cells of the neural retina. Over forty conditions have been associated with CNV [2]. Of these age related macular degeneration (AMD) is the most prevalent.

AMD is the most common cause of severe visual loss in the developed world, impairing more than 10 million people in the United States alone [3]. Approximately one in three people over the age of 75 are affected to some degree [4]. Moreover, the US Census Bureau predicts that the number of people in this age group will increase by 60-80% in the next 25 years, making the prevalence of blindness from AMD greater than glaucoma and diabetic retinopathy combined. The vast majority of patients with AMD who suffer from legal blindness are affected with the neovascular form of the condition. It is estimated that 90% of eyes with severe vision loss due to AMD have CNV [5], underscoring the fact that, although it affects only a fraction of all AMD patients, CNV is the major cause of vision loss in this disease.

The overall visual prognosis for CNV remains dismal. Severe visual loss occurs in over 60% of CNV cases over a five year period [6-8]. In general, the currently available therapeutic modalities are only able to decrease the extent to which vision is lost and are incapable of restoring vision [9-12].

The identification of distinct markers that differentially label components of CNV could yield important insights into the pathogenesis of this condition. The resultant clinical benefit of molecularly targeted treatment of CNV would be significant. In this study, we performed a lectin histochemical assay of choroidal neovascular membranes (CNVMs) from three donors to determine whether a specific carbohydrate composition is associated with the neovascular complex.

Lectin histochemistry is a morphological technique that takes advantage of the carbohydrate binding characteristics of plant, animal and fungal proteins [13]. Different cell types, and cells under different environmental influences, alter their surface carbohydrate composition, and these alterations may be detected histologically or biochemically. This approach has been utilized on eyes with early AMD, to determine compositional characteristics of drusen and basal laminar deposits [14-16].

In this study, we examined the carbohydrate moieties present in CNV and compared the labeling pattern of CNV with normal retinal and choroidal blood vessels. We found that a number of carbohydrate moieties were present on the vascular elements of CNVMs and disciform scars, including those recognized by soybean agglutinin (SBA), *Vicia villosa* agglutinin (VVA), *Ulex europaeus* agglutinin I (UEA-I), and succinyl wheat germ agglutinin (sWGA). SBA and sWGA were found to recognize the vascular elements of CNVMs at concentrations that failed to show strong labeling of normal vessels of the retina and choroid.

## METHODS

Aged donor eyes from three individuals with CNVMs were received from the Iowa Lions Eye Bank (Iowa City, IA). Eye-

---

Correspondence to: Robert F Mullins, 4135E MERF, 375 Newton Road, Iowa City, IA, 52242; Phone: (319) 335-8222; FAX: (319) 335-6641; email: robert-mullins@uiowa.edu

cups or macular punches were either fixed (Cases 1 and 2) or were embedded unfixed (Case 3), as described below. Eyes were fixed by immersion for 2 h in 4% paraformaldehyde solution diluted in 10 mM phosphate buffered saline (PBS), pH 7.4. Eyes were fixed within 5 h of death. Maculae were washed in PBS and were then infiltrated and embedded in sucrose solution [17]. The maculae from these eyes were serially sec-

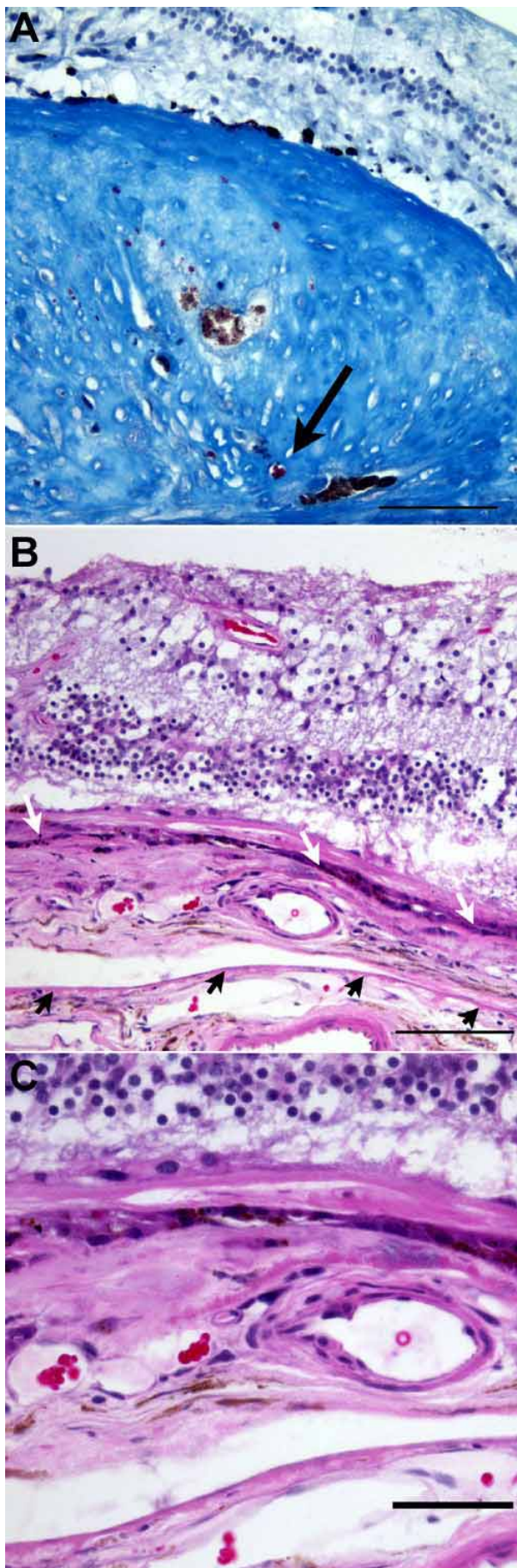
tioned on a Microm HM505E cryostat and employed in the lectin histochemical study. Labeling patterns of the CNVMs in these eyes were compared with the patterns in normal retinal and choroidal endothelial cells (ECs) in these same eyes.

In order to determine whether the sucrose infiltration and embedment affected the pattern of labeling, a third eye with subpigment epithelial CNV (Case 3) was embedded unfixed

TABLE 1. HISTOCHEMISTRY OF CNVMs

Lectin	Specificity	Target	Case 1	Case 2	Case 3
Canavalia ensiformis (Con A)	$\alpha$ -linked mannose	BlamD	+	+	*
		Scar	+	+	*
		CNV BV	+	+	*
Dolichos bifloras (DBA)	$\alpha$ -linked Gal NAc	BlamD	-	-	-
		Scar	-	-	-
		CNV BV	-	$\pm$ subset	-
Arachis hypogea (PNA)	galactosyl ( $\beta$ -1,3) GalNAc	BlamD	-	-	-
		Scar	-	++	$\pm$
		CNV BV	-	+ subset	$\pm$
Glycine max (SBA)	$\alpha$ - or $\beta$ -linked GalNAc	BlamD	-	-	-
		Scar	-	-	-
		CNV BV	+	+	+
Ulex europaeus I (UEA-I)	$\alpha$ -linked fucose	BlamD	-	-	-
		Scar	-	-	-
		CNV BV	+	+	+
			(normal BV+)	(normal BV+)	(normal BV+)
Pisum sativum (PSL)	oligosaccharides with $\alpha$ -linked mannose	BlamD	$\pm$ to +	+	*
		Scar	++	++	*
		CNV BV	$\pm$	+	*
Vicia villosa (VVA)	$\alpha$ - or $\beta$ -linked terminal of GalNAc	BlamD	+	-	-
		Scar	-	$\pm$	-
		CNV BV	$\pm$	+	+
Phaseolus vulgaris (PHA-L)	Complex oligosaccharides	BlamD	-	$\pm$	*
		Scar	-	$\pm$	*
		CNV BV	$\pm$ in scar	+	*
Triticum vulgaris (Succinylated) (sWGA)	GlcNAc	BlamD	$\pm$ (outer)	+	+
		Scar	-	-	-
		CNV BV	+ subset	++	+
Erythrina crisagalli (ECL)	Galactose, esp. gal ( $\beta$ -1,4) GalNAc	BlamD	+ regionally	$\pm$	*
		Scar	-	+	*
		CNV BV	+ in scar	+	*
Sambucus nigra (EBL)	NeuNAc alpha2-6 Gal>NeuNAc alpha2,3 Gal	BlamD	+	+	+
		Scar	+	-	+
		CNV BV	+	$\pm$	High background
			(normal BV+)	(normal BV+)	

Lectins employed in this study, their specificities, and patterns of labeling in three eyes with CNVMs are detailed in the table. Labeling of the disciform scar, basal laminar deposits (BlamD), and the CNV blood vessels is indicated. Labeling patterns are defined as follows: no labeling (-), weak, variable labeling (+/-), consistent labeling (+), and intense labeling (++) . An asterisk indicates that the slide could not be assessed (Case 3 only).



in optimal cutting temperature medium (OCT; Ted Pella; Redding, CA) within 12 h of death. Frozen sections from this donor were evaluated with the same battery of lectins.

Patterns of lectin labeling in two eyes with choroidal neovascularization were evaluated. The panel of biotinylated lectins and their specificities are shown in Table 1. All lectins were obtained from Vector Laboratories (Burlingame, CA). Lectin labeling was performed essentially as described previously [15] except that biotinylated lectins were utilized, followed by detection with avidin-Texas red (Vector Labs). The divalent cations  $MgCl_2$  and  $CaCl_2$  (1 mg/mL each) were included in all steps of the labeling protocol. Sections were blocked for 15 min in PBS with 1 mg/mL bovine serum albumin (Sigma, St. Louis, MO). Sections were then incubated in the biotinylated lectin diluted 1:50 to 1:400 in PBS (with albumin,  $MgCl_2$  and  $CaCl_2$ ) for 30 min, followed by three 5-min washes, and incubation in avidin-Texas red (25  $\mu$ g/mL) and the nuclear counterstain DAPI (4'-6-diamidino-2-phenylindole) for 30 min. Following three 5-min washes in PBS, sections were coverslipped in Aquamount (Lerner Laboratories, Pittsburgh, PA).

Additional sections were stained using conventional hematoxylin/eosin staining (H&E), periodic acid-Schiff (PAS), or Masson's trichrome (MT). PAS and MT staining were performed at the University of Iowa F. C. Blodi Ocular Pathology Laboratory (Iowa City, IA).

Sections were photographed on an Olympus BX41 microscope with a fluorescence attachment and filter sets for fluorescein, rhodamine, and DAPI. In order to discriminate between autofluorescence and Texas red labeling (particularly in areas of RPE lipofuscin, which is highly autofluorescent), all photographed fields were imaged in red, green and blue channels.

Eyes were also labeled with antibodies directed against type IV collagen (Chemicon rabbit polyclonal antibody, Temecula, CA) to visualize vascular basal laminae and with NBT/BCIP (Vector Laboratories) in order to visualize the endogenous alkaline phosphatase activity of endothelial cells [18]. Immunohistochemical labeling was performed as described previously [19].

## RESULTS

The three eyes with neovascular membranes and disciform scars showed features typical of those described in the literature for CNVMs associated with AMD [20-24], reviewed in [25].

Figure 1. Histopathology of Case 1. **A**: Area of disciform scarring reacts with Masson's Trichrome to give a blue staining pattern. Note the RPE pigment and the small vessel with red blood cells embedded in the scar (arrow). The outer nuclear layer shows significant degeneration. The scale bar represents 100  $\mu$ m. **B**: A subpigment epithelial neovascular membrane is present in this eye, with degeneration of the overlying retina. This membrane is primarily located between the dystrophic RPE (white arrows) and Bruch's membrane (black arrows; H&E stain). The scale bar represents 100  $\mu$ m. **C**: Higher magnification of **B** (H&E stain). The scale bar represents 50  $\mu$ m.

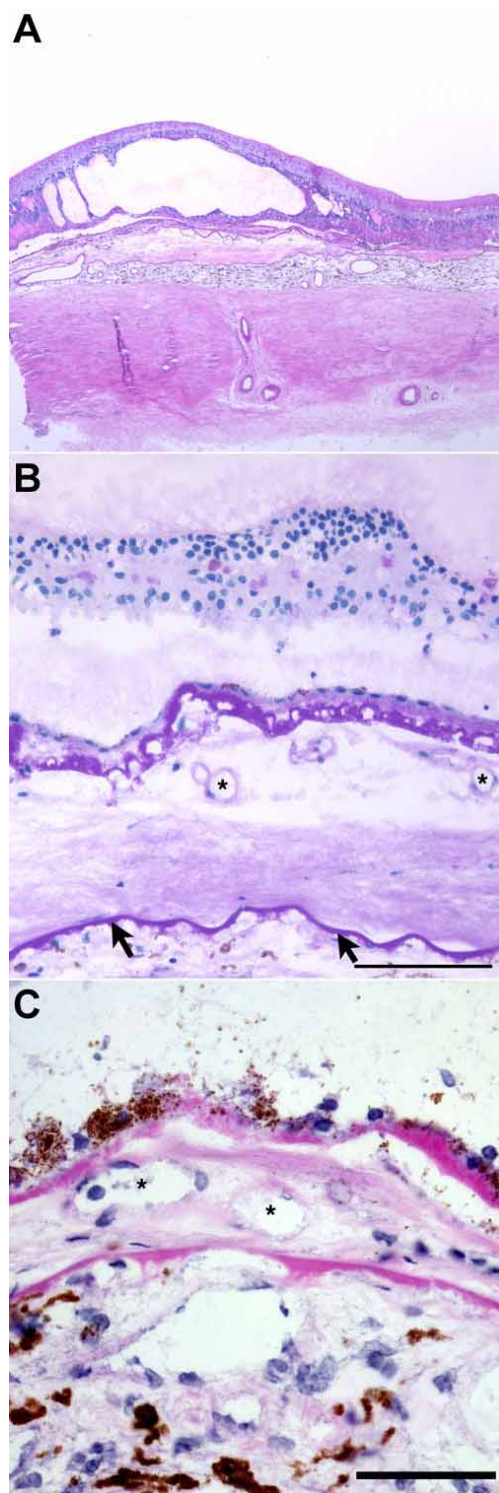


Figure 2. Histopathology of Cases 2 and 3. **A:** Low magnification view of Case 2 showing cystic changes in the neural retina overlying the area of neovascularization. (H&E stain; collected with a 2.5x objective lens) **B:** PAS reactivity of BlamD in Case 2 and the outer layers of Bruch's membrane (arrows). Several vascular elements are present in the space between these two matrices (asterisks), the outer nuclear layer is attenuated, and cystic changes are present within the inner nuclear layer (PAS stain). The scale bar represents 100  $\mu$ m. **C:** In Case 3, a CNVM is observed between the RPE and the outer layers of Bruch's membrane (H&E stain; asterisks identify blood vessels). The scale bar represents 50  $\mu$ m.

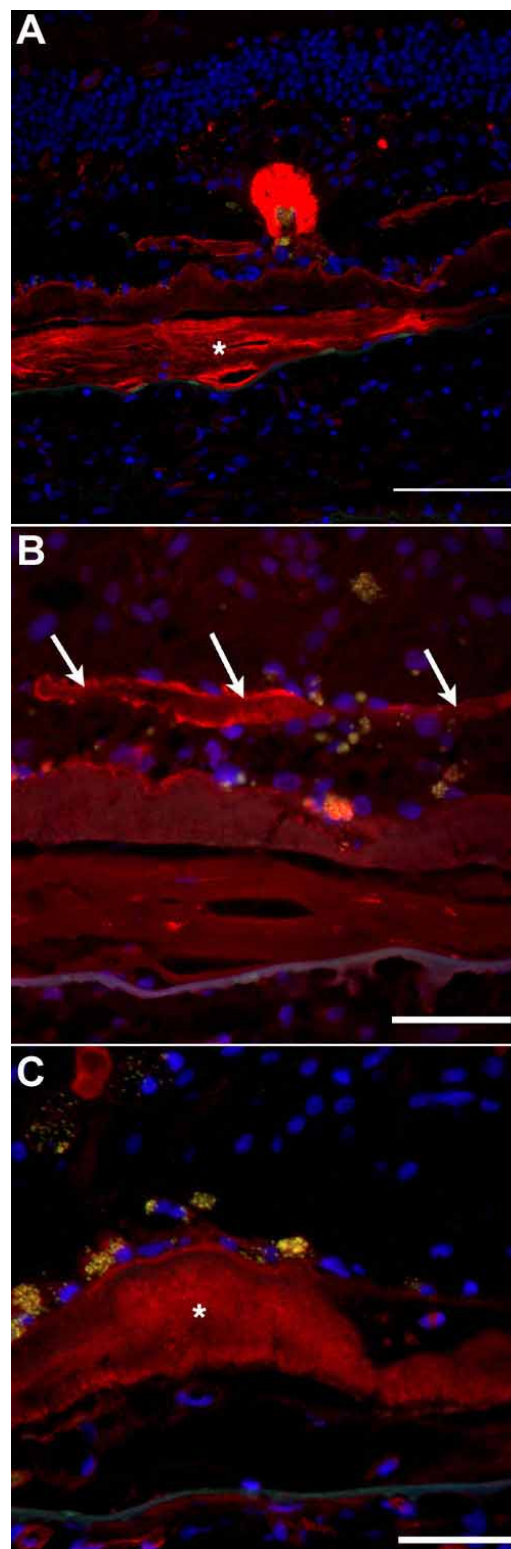


Figure 3. Matrix labeling with some lectins. **A:** PNA labels a photoreceptor rosette (previously described [26]) and the material within the scar (asterisk). **B:** VVA reacts with basement membrane material in the subretinal space (arrows). **C:** When utilized at higher concentrations, sWGA reacts with the layer of basal lamina deposit (asterisk) and choriocapillaris blood vessels. Red fluorescence indicates lectin labeling, blue fluorescence indicates DAPI labeling, and orange-yellow fluorescence indicates RPE lipofuscin autofluorescence. The scale bars represent 100  $\mu$ m in **A** and 50  $\mu$ m in **B,C**.

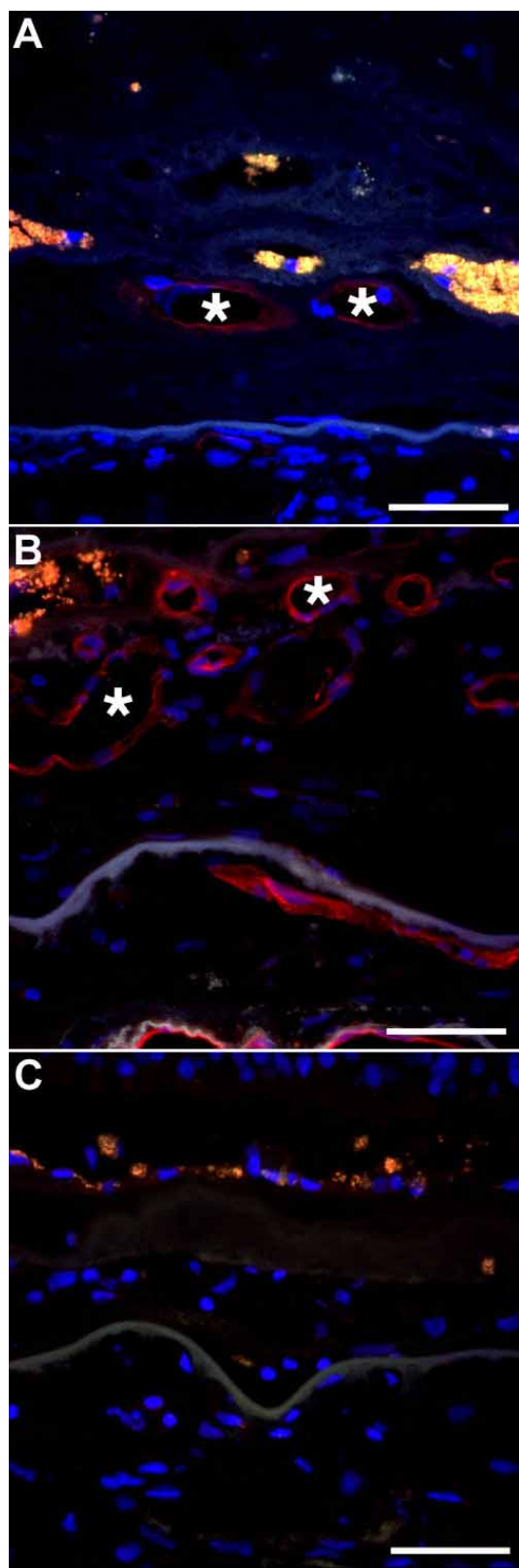


Figure 4. Reaction of choroidal neovessels with the fucose-binding lectin UEA-I. All viable vessels in Case 1 (A) and Case 2 (B) were labeled with UEA-I (asterisks). C: Very minor fluorescence of some vessels was observed with the avidin-Texas red reagent alone (Case 2). The scale bars represent 50  $\mu\text{m}$ . Red fluorescence indicates lectin labeling, blue fluorescence indicates DAPI labeling, and orange-yellow fluorescence indicates RPE lipofuscin autofluorescence.

In Case 1, a large, compact subfoveal scar was noted that was eosinophilic and stained blue on MT stain, suggesting a significant amount of collagen (Figure 1A). The scar contained fibrovascular material that was present on both sides of a detached layer of basal laminar deposit with a discontinuous RPE layer on its inner surface. Islands of RPE were noted within the scar, as were rare vessels (Figure 1A). Photoreceptor degeneration was noted above the scar, and several rosettes were present in the overlying retina. At the temporal edge of the scar, a flat layer of active blood vessels was noted lying between the outer aspect of Bruch's membrane and the degenerated RPE (Figure 1B,C).

In Case 2, a two-layered CNVM was present. The retina overlying the CNVM exhibited severe cystic changes at the level of the inner nuclear layer (Figure 2A). In addition, the outer nuclear layer and photoreceptor outer segments were extremely attenuated. A detached layer of meandering basal laminar deposit (BlamD) was also noted, with a layer of loose proteinaceous material between the outer layers of Bruch's membrane and the layer of BlamD [22] (Figure 2B). PAS-reactive material in the BlamD and the residual Bruch's membrane was observed, with active blood vessels and matrix elements occupying this space (Figure 2B). Case 3, an unfixed eye with a comparatively long death-preservation time, showed similar characteristics, except that the CNVM was located only in the subpigment epithelial space, between a layer of BlamD and Bruch's membrane (Figure 2C).

The labeling patterns of eleven lectins were determined in the retinal blood vessels, choroidal blood vessels, the glycoconjugates within the scar, and the vascular components of the neovascular membrane. The observed patterns are described in Table 1 and in Figure 3, Figure 4, Figure 5, and Figure 6.

Several lectins showed intense labeling of matrix elements within the CNVM and/or disciform scar. The material within the scar was labeled with PNA (in Case 2 only; Figure 2A) and PSL (in Cases 1 and 2). A sheet of matrix in the subretinal space, most likely corresponding to the basal lamina of dystrophic RPE cells, was labeled with SBA, PNA, and VVA (Figure 3B). When used at higher concentrations (20  $\mu\text{g}/\text{mL}$ ), sWGA labeled basal laminar deposits (Figure 3C). At this concentration, sWGA also labeled normal retinal and choroidal vasculature. PNA also labeled photoreceptor rosettes, which were observed in the overlying retina, as described previously (Figure 3A) [26].

Vessels in the CNVM were labeled with UEA-I (which labeled all vessels in the eyes studied, Figure 4A,B). Reactivity of the CNVM vessels was also noted with VVA (Figure 5A), PSL, SBA (Figure 5B,C), and sWGA (Figure 5D). These probes also showed variable labeling of vessels in normal retina and/or choroid. SBA was notably higher in CNV vessels in Case 2 than in normal retinal and choroidal vessels, and exhibited positive reactivity of these vessels at relatively low concentrations (2.5  $\mu\text{g}/\text{mL}$ ) that did not label other structures in the eye. Similarly, sWGA labeled choroidal neovessels at concentrations at which other vascular beds were unlabeled or very weakly labeled. Similar results were obtained between

sucrose embedded (Cases 1 and 2) and unfixed (Case 3) CNVMs (Table 1).

We also sought to evaluate the glycoconjugates associated with a large feeder vessel breaching Bruch's membrane in Case 2 (Figure 6A). Two lectins found to react with subpigment epithelial vessels in CNV were utilized in dual labeling experiments with an antibody directed against type IV collagen. Both SBA (Figure 6B) and sWGA (Figure 6C) reacted with components of this large vessel. The SBA-reactive glycoconjugates appeared to be external to the inner layer

of ECs, whereas sWGA appeared to localize to the EC surface internal to the layer of collagen IV (Figure 6C).

## DISCUSSION

Endothelial cells express a broad spectrum of glycoconjugates that differ between species, between types of vessels, and between ECs in healthy and diseased states. Changes in the distribution of EC carbohydrate surface molecules have been described in several pathologic conditions, including experimental abdominal cryptorchidism [27], normal and dystrophic

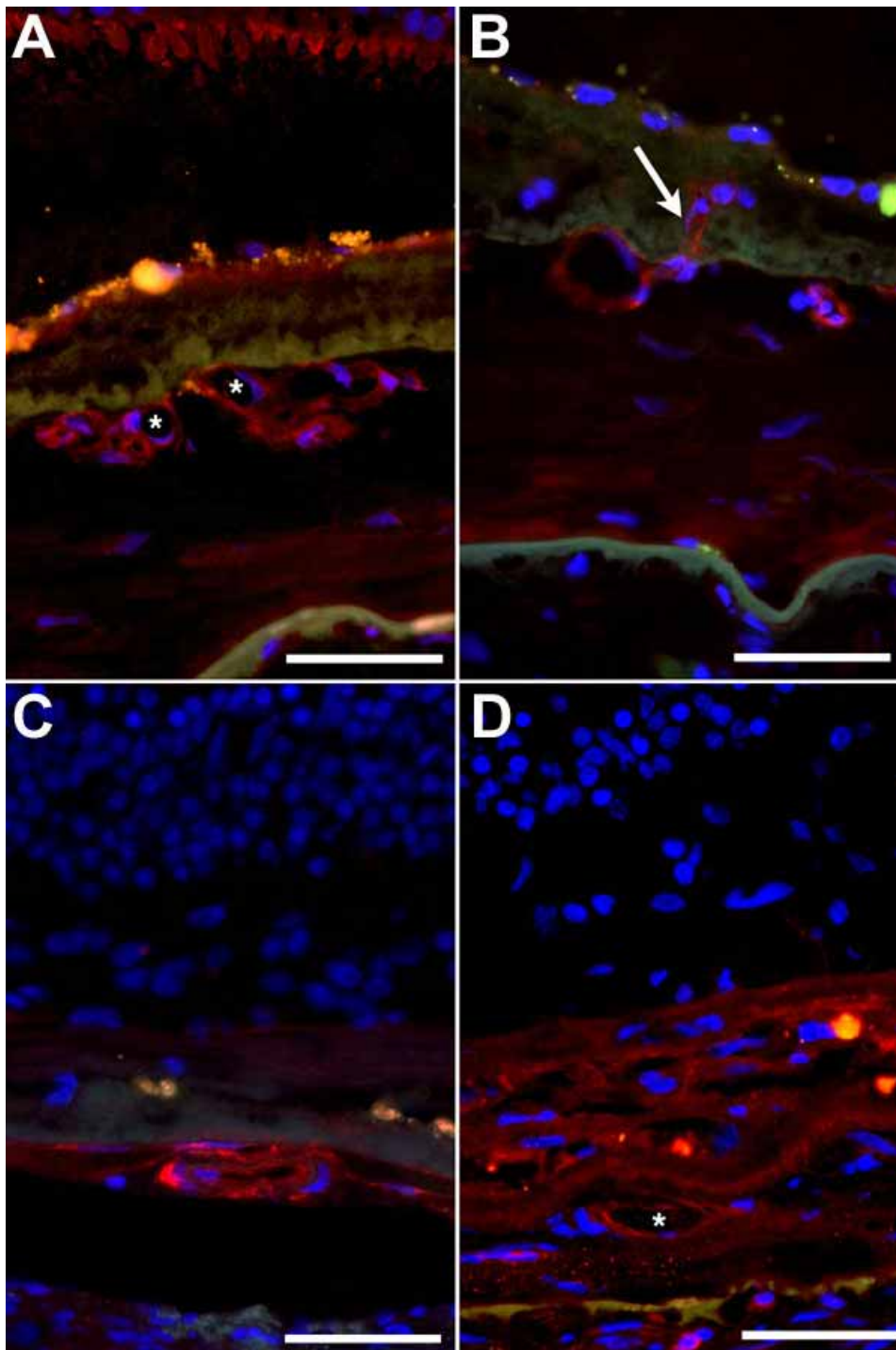


Figure 5. Lectin reactivity of vessels in choroidal neovascular membranes. **A:** VVA labeling of cone inner segments and CNV vasculature (Case 2). **B:** An SBA-reactive vessel in a CNVM sends a branch (arrow) into the layer of Bruch's membrane (Case 2). **C:** A flat layer of vessels in Case 1 is positive for SBA. **D:** Vessels in Case 1 reactive for sWGA (asterisk). Red fluorescence indicates lectin labeling, blue fluorescence represents DAPI labeling, and orange-yellow fluorescence indicates RPE lipofuscin autofluorescence. The scale bars represent 50  $\mu$ m.

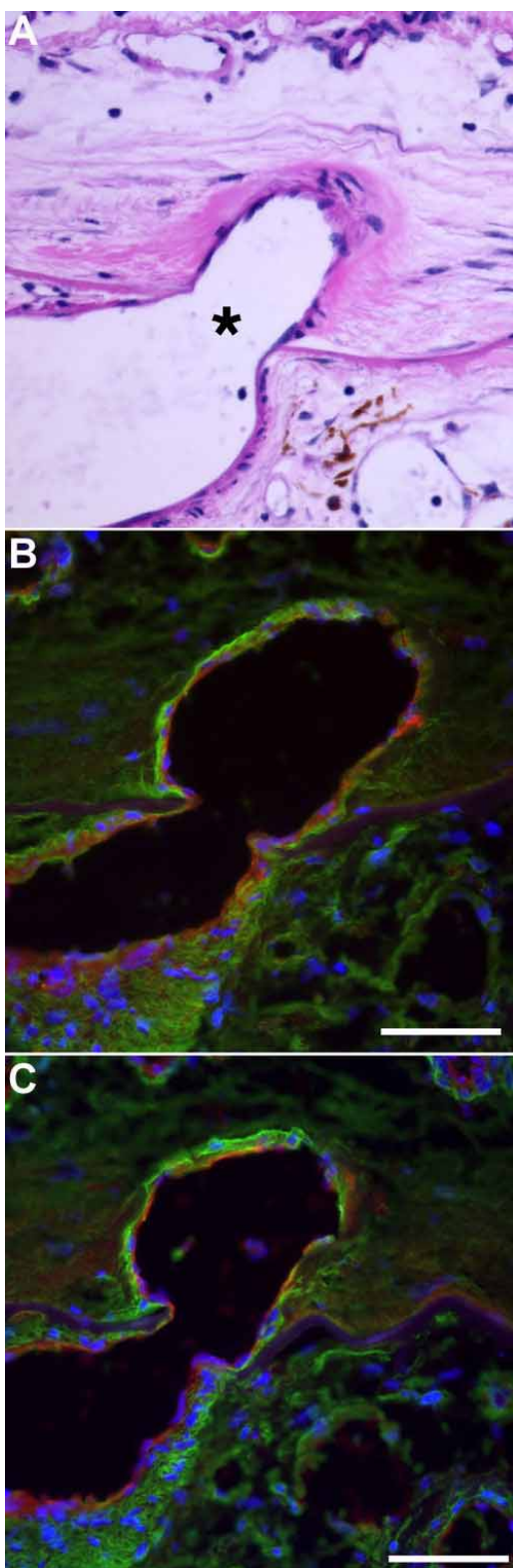


Figure 6. Histochemistry of a feeder vessel in a CNVM. **A:** Hematoxylin and eosin stain of a large vessel breaching Bruch's membrane (at the asterisk). **B:** Colocalization of collagen type IV (green) and SBA (red) in this vessel. Note the reactivity of SBA in the endothelium and surrounding matrix. **C:** Colocalization of collagen type IV (green) and sWGA (red) in the same vessel shown in **A** and **B**. Note that, unlike SBA, most of the sWGA binding is present on the endothelium. All scale bars represent 50  $\mu$ m.

umbilical cord vasculature [28], and experimentally-injured brain microvascular ECs [29].

In addition, several studies have also shown that ECs in angiogenic and migrating states may express a different set of cell surface carbohydrate moieties than quiescent ECs. Studies on chicken chorioallantoic membrane ECs during normal vascular development [30] and on migrating cultured aortic ECs following experimental debridement [31] have shown that the lectin-binding profile of ECs changes during growth and migration. Glycoconjugates containing N-acetyl-glucosamine (GlcNAc) were found to be upregulated in both cases. Interestingly, vessels in choroidal neovascular membranes were also found to react intensely with sWGA, a marker for GlcNAc-containing oligosaccharides. Whether these reactive carbohydrates are components of glycoproteins or glycolipids can not be readily determined by lectin histochemistry, and evaluating the biochemical nature of these glycoconjugates will be an interesting extension of these studies.

Although relatively little is understood about the biochemistry of CNV ECs, recent studies have begun to explore the expression of EC markers in human and animal CNVMs. Immunolabeling of CNVMs has shown that endoglin/CD105 is associated with CNV ECs [32,33], and adhesion molecules such as ICAM-1/CD54 and E-selectin are present in human [34] and experimental [35] choroidal neovascularization. Endothelial cells in a mouse model of CNV have been shown to react with *Lycopersicon esculentum* agglutinin [36], a lectin from tomato with affinity for GlcNAc oligomers. In our hands, this lectin did label rosettes and CNVMs in Case 2, but did not show strong specificity for CNV over normal vessels or other matrix elements (data not shown). Lectin reactivities of blood vessels differ significantly among mammalian species [37], and it will be interesting to determine the similarities in the glycoconjugate profiles of mouse experimental CNV and human CNV.

Although the function of altered EC oligosaccharide chains in CNV remains unclear, there are several steps in the process of CNV formation in which glycosylation is likely to play a role. Angiogenesis is regulated in part by the interactions of matrix metalloproteinases (MMPs) and their substrates [38]. Mutations in TIMP3, a regulator of metalloproteinases, result in a form of macular dystrophy that can be complicated by CNV [39,40]. Recently it has been shown that some members of the MMP family of enzymes modulate their interactions based upon their glycosylation state [41]. Moreover, endothelial cell activation molecules such as ICAM-1, which is required for CNV formation in the murine model of CNV [42] and which is localized to CNVMs in human eyes [34], have functions that similarly rely on a specific state of glycosylation [43].

In the current study we describe the localization of a battery of lectins to CNVMs in human eyes. There are a number of limitations in the current study. The patterns of lectin labeling were evaluated in only a small number of eyes. In addition, the eyes used in this study had disciform scars, an end stage cicatricial response in CNV. It is possible that eyes with earlier staged CNV might reveal a different set of carbohy-

drate moieties. Whether abnormal vessels assayed at various stages of CNV maturation would demonstrate different glycoconjugate profiles is an interesting and open question. We did find, however, that SBA (a lectin from the soybean *Glycine max*) and sWGA (succinylated wheat germ agglutinin) label CNV endothelial cells. Significantly, these lectins reacted with the abnormal microvasculature in CNV at concentrations at which labeling of normal retinal and choroidal vasculature was absent or markedly reduced, which suggests that CNV ECs may possess specific glycoconjugates. The identification of the glycoconjugate profile of the abnormal vessels in CNV may be useful in understanding the pathophysiology of CNV.

#### ACKNOWLEDGEMENTS

Supported in part by RO3 EY14563 (RFM), a Carver Trust Medical Research Initiative Grant (RFM); and the Heed Foundation (MAG). The authors wish to thank Elizabeth Malone and Marissa Olvera for technical assistance, and Dr. Nasreen Syed and Christy Ballard for their assistance with special staining techniques, and the Iowa Lions Eye Bank for procuring the human donor eyes used in this study. A patent application based on this work has been filed.

#### REFERENCES

- Gass JD. Drusen and disciform macular detachment and degeneration. *Arch Ophthalmol* 1973; 90:206-17.
- Green WR, Wilson DJ. Choroidal neovascularization. *Ophthalmology* 1986; 93:1169-76.
- Friedman DS, O'Colmain BJ, Munoz B, Tomany SC, McCarty C, de Jong PT, Nemesure B, Mitchell P, Kempen J, Eye Diseases Prevalence Research Group. Prevalence of age-related macular degeneration in the United States. *Arch Ophthalmol* 2004; 122:564-72.
- Klein R, Klein BE, Linton KL. Prevalence of age-related maculopathy. The Beaver Dam Eye Study. *Ophthalmology* 1992; 99:933-43.
- Ferris FL 3rd, Fine SL, Hyman L. Age-related macular degeneration and blindness due to neovascular maculopathy. *Arch Ophthalmol* 1984; 102:1640-2.
- Visual outcome after laser photocoagulation for subfoveal choroidal neovascularization secondary to age-related macular degeneration. The influence of initial lesion size and initial visual acuity. Macular Photocoagulation Study Group. *Arch Ophthalmol* 1994; 112:480-8.
- Laser photocoagulation for juxtafoveal choroidal neovascularization. Five-year results from randomized clinical trials. Macular Photocoagulation Study Group. *Arch Ophthalmol* 1994; 112:500-9.
- Argon laser photocoagulation for neovascular maculopathy. Five-year results from randomized clinical trials. Macular Photocoagulation Study Group. *Arch Ophthalmol* 1991; 109:1109-14. Erratum in: *Arch Ophthalmol* 1992; 110:761.
- Bressler NM, Treatment of Age-Related Macular Degeneration with Photodynamic Therapy (TAP) Study Group. Photodynamic therapy of subfoveal choroidal neovascularization in age-related macular degeneration with verteporfin: two-year results of 2 randomized clinical trials-tap report 2. *Arch Ophthalmol* 2001; 119:198-207.
- Gragoudas ES, Adamis AP, Cunningham ET Jr, Feinsod M, Guyer DR, VEGF Inhibition Study in Ocular Neovascularization Clinical Trial Group. Pegaptanib for neovascular age-related macular degeneration. *N Engl J Med* 2004; 351:2805-16.
- Ferris FL 3rd. A new treatment for ocular neovascularization. *N Engl J Med* 2004; 351:2863-5.
- Bressler NM. Age-related macular degeneration is the leading cause of blindness... *JAMA* 2004; 291:1900-1.
- Danguy A, Decaestecker C, Genten F, Salmon I, Kiss R. Applications of lectins and neoglycoconjugates in histology and pathology. *Acta Anat (Basel)* 1998; 161:206-18.
- Kliffen M, Mooy CM, Luider TM, de Jong PT. Analysis of carbohydrate structures in basal laminar deposit in aging human maculae. *Invest Ophthalmol Vis Sci* 1994; 35:2901-5.
- Mullins RF, Johnson LV, Anderson DH, Hageman GS. Characterization of drusen-associated glycoconjugates. *Ophthalmology* 1997; 104:288-94.
- Mullins RF, Hageman GS. Human ocular drusen possess novel core domains with a distinct carbohydrate composition. *J Histochem Cytochem* 1999; 47:1533-40.
- Barthel LK, Raymond PA. Improved method for obtaining 3-microns cryosections for immunocytochemistry. *J Histochem Cytochem* 1990; 38:1383-8.
- McLeod DS, Luty GA. High-resolution histologic analysis of the human choroidal vasculature. *Invest Ophthalmol Vis Sci* 1994; 35:3799-811.
- Mullins RF, Russell SR, Anderson DH, Hageman GS. Drusen associated with aging and age-related macular degeneration contain proteins common to extracellular deposits associated with atherosclerosis, elastosis, amyloidosis, and dense deposit disease. *FASEB J* 2000; 14:835-46.
- Small ML, Green WR, Alpar JJ, Drewry RE. Senile macular degeneration. A clinicopathologic correlation of two cases with neovascularization beneath the retinal pigment epithelium. *Arch Ophthalmol* 1976; 94:601-7.
- Green WR, McDonnell PJ, Yeo JH. Pathologic features of senile macular degeneration. *Ophthalmology* 1985; 92:615-27.
- Bressler SB, Silva JC, Bressler NM, Alexander J, Green WR. Clinicopathologic correlation of occult choroidal neovascularization in age-related macular degeneration. *Arch Ophthalmol* 1992; 110:827-32.
- Sarks JP, Sarks SH, Killingsworth MC. Morphology of early choroidal neovascularisation in age-related macular degeneration: correlation with activity. *Eye* 1997; 11:515-22.
- Grossniklaus HE, Cingle KA, Yoon YD, Ketkar N, L'Hernault N, Brown S. Correlation of histologic 2-dimensional reconstruction and confocal scanning laser microscopic imaging of choroidal neovascularization in eyes with age-related maculopathy. *Arch Ophthalmol* 2000; 118:625-9.
- Green WR. Histopathology of age-related macular degeneration. *Mol Vis* 1999; 5:27.
- Rayborn M, Myers K, Hollyfield J. Photoreceptor rosettes in age-related macular degeneration donor tissues. In: LaVail MM, Hollyfield JG, Anderson RE, editors. *Degenerative retinal diseases*. New York: Plenum Press; 1997. p. 17-21.
- Pinart E, Bonet S, Briz MD, Pastor LM, Sancho S, Garcia N, Badia E. Morphologic and histochemical study of blood capillaries in boar testes: effects of abdominal cryptorchidism. *Teratology* 2001; 63:42-51.
- Sgambati E, Brizzi E, Marini M, Gheri Bryk S, Gheri G. Lectin binding in the human umbilical cord from normally grown pregnancies and from pregnancies complicated by intra-uterine growth retardation with absent or reversed diastolic flow. *Biol Neonate* 2003; 84:119-34.

29. Vorbrodt AW. Changes in the distribution of endothelial surface glycoconjugates associated with altered permeability of brain micro-blood vessels. *Acta Neuropathol (Berl)* 1986; 70:103-11.
30. Henry CB, DeFouw DO. Differential lectin binding to microvascular endothelial glycoconjugates during normal angiogenesis in the chick chorioallantoic membrane. *Microvasc Res* 1995; 49:201-11.
31. Augustin-Voss HG, Pauli BU. Migrating endothelial cells are distinctly hyperglycosylated and express specific migration-associated cell surface glycoproteins. *J Cell Biol* 1992; 119:483-91.
32. Yasukawa T, Kimura H, Tabata Y, Miyamoto H, Honda Y, Ikada Y, Ogura Y. Active drug targeting with immunoconjugates to choroidal neovascularization. *Curr Eye Res* 2000; 21:952-61.
33. Grisanti S, Canbek S, Kaiserling E, Adam A, Lafaut B, Gelisken F, Szurman P, Henke-Fahle S, Oficjalska-Mlynczak J, Bartschmidt KU. Expression of endoglin in choroidal neovascularization. *Exp Eye Res* 2004; 78:207-13.
34. Yeh DC, Bula DV, Miller JW, Gragoudas ES, Arroyo JG. Expression of leukocyte adhesion molecules in human subfoveal choroidal neovascular membranes treated with and without photodynamic therapy. *Invest Ophthalmol Vis Sci* 2004; 45:2368-73.
35. Shen WY, Yu MJ, Barry CJ, Constable IJ, Rakoczy PE. Expression of cell adhesion molecules and vascular endothelial growth factor in experimental choroidal neovascularisation in the rat. *Br J Ophthalmol* 1998; 82:1063-71.
36. Csaky KG, Baffi JZ, Byrnes GA, Wolfe JD, Hilmer SC, Flippin J, Cousins SW. Recruitment of marrow-derived endothelial cells to experimental choroidal neovascularization by local expression of vascular endothelial growth factor. *Exp Eye Res* 2004; 78:1107-16.
37. Alroy J, Goyal V, Skutelsky E. Lectin histochemistry of mammalian endothelium. *Histochemistry* 1987; 86:603-7.
38. Anand-Apte B, Pepper MS, Voest E, Montesano R, Olsen B, Murphy G, Apte SS, Zetter B. Inhibition of angiogenesis by tissue inhibitor of metalloproteinase-3. *Invest Ophthalmol Vis Sci* 1997; 38:817-23.
39. Weber BH, Vogt G, Pruett RC, Stohr H, Felbor U. Mutations in the tissue inhibitor of metalloproteinases-3 (TIMP3) in patients with Sorsby's fundus dystrophy. *Nat Genet* 1994; 8:352-6.
40. Wong SC, Fong KC, Lee N, Gregory-Evans K, Gregory-Evans CY. Successful photodynamic therapy for subretinal neovascularisation due to Sorsby's fundus dystrophy: 1 year follow up. *Br J Ophthalmol* 2003; 87:796-7.
41. Wu YI, Munshi HG, Sen R, Snipas SJ, Salvesen GS, Fridman R, Stack MS. Glycosylation broadens the substrate profile of membrane type 1 matrix metalloproteinase. *J Biol Chem* 2004; 279:8278-89.
42. Sakurai E, Taguchi H, Anand A, Ambati BK, Gragoudas ES, Miller JW, Adamis AP, Ambati J. Targeted disruption of the CD18 or ICAM-1 gene inhibits choroidal neovascularization. *Invest Ophthalmol Vis Sci* 2003; 44:2743-9.
43. Jimenez D, Roda-Navarro P, Springer TA, Casasnovas JM. Contribution of N-linked glycans to the conformation and function of intercellular adhesion molecules (ICAMs). *J Biol Chem* 2005; 280:5854-61.